Surface Accuracy Analysis of Single Panels for the Shanghai 65-M Radio Telescope

LI FU
Shanghai Astronomical Observatory, Chinese Academy of Sciences, Shanghai
CHINA
Key Laboratory of Radio Astronomy, Chinese Academy of Sciences, Nanjing
CHINA

GUOXI LIU, CHAO JIN, FENG YAN
54th Research Institute of China Electronics Technology Group Corporation, Shijiazhuang
CHINA

TAO AN, ZHIQIANG SHEN
Shanghai Astronomical Observatory, Chinese Academy of Sciences, Shanghai
CHINA
Key Laboratory of Radio Astronomy, Chinese Academy of Sciences, Nanjing
CHINA

fuli@shao.ac.cn

Abstract: - We presented the surface accuracy measurements of 5 single panels of the Shanghai 65-meter radio telescope by employing the coordinate measuring machine and laser tracker. The measurement data obtained from the two instruments were analyzed with the common point transformation and CAD surface fitting techniques, respectively. The derived rms uncertainties of panel accuracy from two methods are consistent with each other, and both match the design specification. The simulations of the effects of manufacturing error, gravity, temperature and wind on the panel surface accuracy with the finite element analysis method suggest that the first two factors account for primary sources of the accuracy uncertainty. The panel deformation under concentrated load was analyzed through finite element analysis and experiment, and the comparison error is 5.6%. There is not plastic deformation when people of weight below 70kg installs and remedies the panel.

Key-Words: - antennas, finite element methods, measurement, accuracy, panel

1. Introduction

The surface of a large millimeter-wavelength radio telescope has to be measured and calibrated to a very high accuracy in order to guarantee a high efficiency. The largest solid-panel radio telescopes in the world, the Robert C. Byrd Green Bank Telescope (GBT) of the US, the Effelsberg radio telescope of the Germany, the Sardinia Radio Telescope (SRT) of the Italy, and the Shanghai 65-meter Radio Telescope (in brief, Sh65RT hereafter) of the China, are all composed of high-accuracy panels.

The GBT is a 100-meter diameter offset-paraboloid Gregorian reflector radio telescope operating in the frequency range from 290MHz to 100GHz. The primary reflector consists of 2004 small trapezoidal shaped panels (on average, 3.9m2 each) and the average accuracy of individual panels is 68μm [1].

The Effelsberg 100-meter radio telescope works in the frequency range from 0.3 to 95.5GHz. The primary reflector consists of 2353 panels and the overall mirror surface accuracy is slightly less than 0.5mm. The inner cycles (diameter < 60m) are made of aluminum honeycomb panels, and the rms (root mean square) deviations of this honeycomb-type sector give a mean value of 0.22mm. The intermediate diameter range of 60-85m is composed of aluminum “cassette” panel and the rms is 0.27mm. The outer rings (diameter > 85m) are made up of stainless steel mesh with thickness of 6 mm^2,

and the surface deviations are up to 0.55mm (rms) [2].

The SRT is a shaped Gregorian 64-meter radio telescope recently completed in Sardinian Island in Italy. The frequency band continuously covers from 300MHz to 100GHz. The primary mirror composed of 1008 panels distributed on 14 rings [3]. The manufacturing error of individual panel is about 65μm, the thermal-induced error 11μm, the gravity-induced error 29μm and the wind-induce error 4μm [4].

GBT and Effelsberg radio telescopes have achieved a lot of profound-impact scientific results [5,6] and SRT is conducting commissioning observations [7]. All these advanced sciences depend on high-sensitivity observations which in turn rely on the large high-accuracy reflectors. Although the generic antenna structure design [8], overall reflector accuracy and alignment of panels [9] are important for maintaining the perfect parabolic surface, the surface accuracy of single panels is also of essential importance. In this paper, we report the surface accuracy measurements of single panels of the Sh65RT. The two different measurement methods and the data processing methods are described in section 2. In section 3, the measurement data combined to the finite element analysis (FEA) data are used to calculate the rms value of the manufacturing error using the common point coordinate transformation and CAD surface fitting techniques. The effects of manufacturing error, gravity, temperature and wind on panel precision are evaluated with the FEA method. We also discuss the effect of concentrated load on panel deflection in section 4.

2. Measurements and Data Analysis of Panel Surface Accuracy

2.1 Measurement methods

The panel surface accuracy of Sh65RT was measured independently with two different instruments and techniques, the coordinate measuring machine and laser tracker.

2.1.1 Coordinate measuring machine

The primary reflector of the Sh65RT showed in Figure 1 consists of 1008 panels distributed in 14 rings. The targets to measure are from different sectors of the shaped reflector surface and the largest area is about 5m^2. As shown in Figure 2, the panel is formed by steel frame supporting the aluminum sheet, and is placed on four supports. Before the measurements, the panels have been placed in a room with constant temperature (20℃) for longer than eight hours.

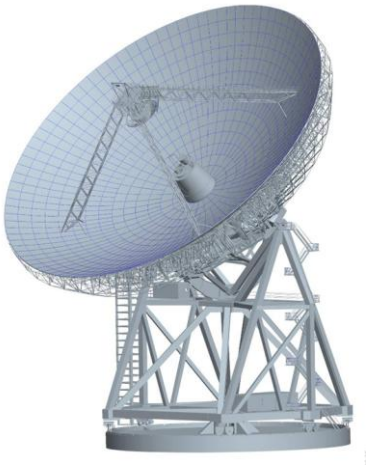

Fig. 1 The 3D model of Sh65RT

First we used coordinate measuring machine (CMM) for the panel surface accuracy measurement. According to the dimension of the single panel and accuracy required, ALPHA IMAGE 25.50.18 CMM was adopted. The work environment temperature of this instrument is 20℃ and the precision is (8.0+8.0L/1000)μm.

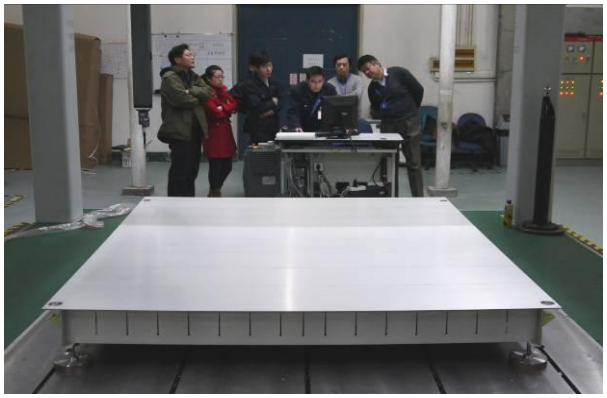

Fig. 2 The measurement of panel under CMM.

Ideally, we set four panel corners to the designed paraboloid by adjusting the supporting screws near each corner so as to separate the panel error from the backup structure (BUS) error. But, a different way to accept a panel is to measure the panel in the factory. We need to duplicate what we define above. First, we established the panel coordinate system. Reference surface is defined by four corner points close to the installing holes. The y axis is perpendicular to the reference surface. One side of the panel was projected on the reference surface to form the *z* axis. The coordinate origin is set to a point on the line connecting z axis and y axis. Next, we switched the reflector coordinate system to the panel coordinate system. The four corner points were repeatedly measured and adjusted to ensure

that all four corners fell at y=0. Finally, according to the preassigned points on the ideal model, operators manually controlled the CMM to determine the relative positions of other measuring points.

2.1.2 Laser tracker

Laser tracker is a portable precision metrology tool enabling to achieve accuracy as high as 5μm/m. The T3-60 system was adopted in our measurements. It composes of a laser tracker and a spherically mounted retroreflector which emits the laser beam.

As shown in Figure 3, the same panels used in above experiment were measured by the laser tracker under the same work environment. The positions of spherically mounted retroreflector are the measuring points which obey the principle of distribution of equal areas and the distance of two consecutive points is between 50mm and 100mm.

Firstly, we set reasonable position between the laser tracker and panel. After the instrumentation turned on for half an hour, the panel can be measured. The environment temperature and pressure during preheating were recorded. The four corner points were also repeatedly measured and adjusted to ensure the corner points lie on a same plane. More than 400 points have been measured.

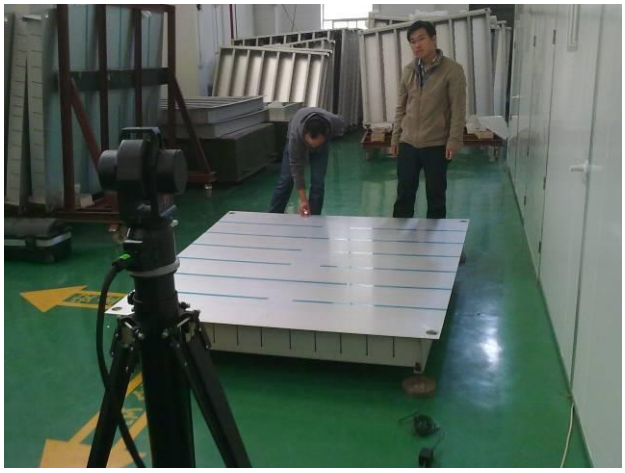

Fig. 3 The measurement of panel under Laser Tracker.

2.2 Data processing

Figure 4 displays the flow chart of the data processing. The data measured from the CMM and Laser track were analyzed separately. In the common point coordinate transformation [10], the measurement data obtained from the CMM were converted from the panel coordinate system to the theoretical coordinate system. The reference points are the four corner points and their positional errors are approximately zero. Comparison between the measurement values obtained by a CMM and a solid model of the panel produces the deviations of Δx, Δy and Δz and the error was calculated with (1).

$$\delta = \sqrt{\Delta x^2 + \Delta y^2 + \Delta z^2} \quad (1)$$

The accuracy of the panel surface is expressed with the rms value of the measuring errors at each point. That is

$$\sigma = \sqrt{\sum_{i=1}^{n} (\delta_i - \bar{\delta})^2 / n} \quad (2)$$

where δ_i is the measuring error of each sampling point, $\bar{\delta}$ the average value, n the number of the points.

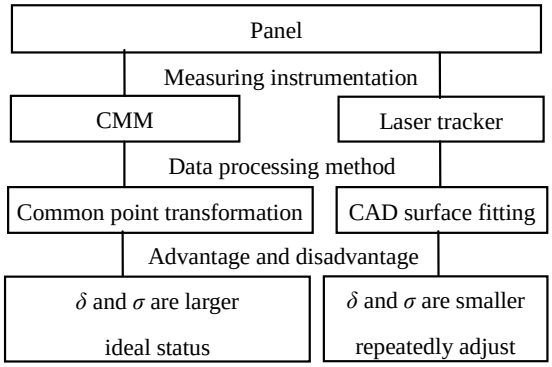

Fig. 4 Illustration of the measurement and data processing method for the individual panel.

The data process of the laser tracker made use of the CAD surface fitting method [11]. The CAD surface model and measuring data were compared and adjusted in order to determine the approximate coordinate transformation parameters. Once these transformation parameters were found, the software calculated automatically and stopped until the square sum of the distance between measuring point and its projection reaches the minimum. This method does not solve the errors of four corner points but is sensitive to the minimization of the square sum of the errors.

Normally the CAD surface fitting method places the origin of the measuring coordinate system in the mirror or panel center. If one wants to obtain the results associated with four corner points, the following steps are adopted:

(i) establishing the panel coordinate system according to three corner points;

(ii) transforming the measuring coordinate system to panel coordinate system;

(iii) converting the panel coordinate to theoretical coordinate system;

(iv) calculating the error of each measuring point and rms value.

As shown in Figure 5, *oxyz* and *o'x'y'z'* represent

the measuring and panel coordinate system, respectively. The three corner points are $P_1(x_1,y_1,z_1)$, $P_2(x_2,y_2,z_2)$ and $P_3(x_3,y_3,z_3)$. The x' axis is defined by the unit vector of P_1P_2. The z' axis is defined by the cross product of vectors P_1P_2 and P_1P_3. In a similar way, the y' axis (P_1P_4) is also established

$$\hat{x}' = \frac{x_2 - x_1}{l_0}\hat{x} + \frac{y_2 - y_1}{l_0}\hat{y} + \frac{z_2 - z_1}{l_0}\hat{z} = P_{xx}\hat{x} + P_{xy}\hat{y} + P_{xz}\hat{z} \quad (3)$$

As a result, the transformation matrix from measuring coordinate system to panel coordinate system is given by

$$\begin{bmatrix} x' \\ y' \\ z' \end{bmatrix} = \begin{bmatrix} P_{xx} & P_{xy} & P_{xz} \\ P_{xy} & P_{yy} & P_{yz} \\ P_{zx} & P_{zy} & P_{zz} \end{bmatrix} \begin{bmatrix} x - x_1 \\ y - y_1 \\ z - z_1 \end{bmatrix} = A \begin{bmatrix} x - x_1 \\ y - y_1 \\ z - z_1 \end{bmatrix} \quad (4)$$

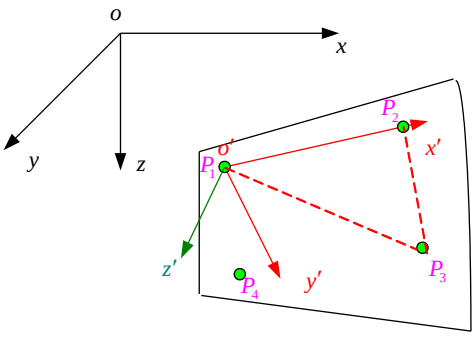

Fig. 5 Schematic of the measuring coordinate system *oxyz* and panel coordinate system *o'x'y'z'*.

2.3 Results and conclusions

All together five panels from different rings have been measured using the CMM and Laser Tracker. The rms uncertainty σ and mean measurement error $\bar{\delta}$ are shown in Figure 6. We should note that σ includes both the manufacturing and gravity-induced errors. The absolute values of $\bar{\delta}_{CMM}$ of five panels are in the range of 0.01~0.08mm. The average value of $\bar{\delta}_{LT}$ is approximately zero since the CAD surface fitting ensures the square sum of error to be minimized, therefore $\bar{\delta}_{LT}$ is not shown in Figure 6. The rms uncertainties σ_{LT} and σ_{CMM} of the five panels were calculated from (2), ranging between 0.07 and 0.09mm. The deviations between two measurements are rather small, indicating that both measurements satisfy the design specification (σ_s<0.10mm: 1st-10th ring; σ_s<0.13mm: 11th-14th ring), and either method is applicable for measuring panel surface smoothness with high accuracy. The largest deviation ($(\sigma_{LT}-\sigma_{CMM})/\sigma_{LT}$~12.5%,) is associated with panel 11-21, probably resulted from large local mechanical errors in certain positions.

We specially investigated the 2-dimensional distribution of the measuring errors in the panel 11-21 (Figure 7). Figure 7(a) shows the CMM measurement errors. It is obviously that in most parts δ_i is rather smooth in the range of $\pm$0.05mm. The large errors (denoted with red color) only appear at a few isolated positions, and the largest one in the left edge. Figure 7(b) shows the distribution of laser track errors. It agrees with the CMM errors in Figure 7(a) in a gross manner. The most significant errors are concentrated close to the left edge.

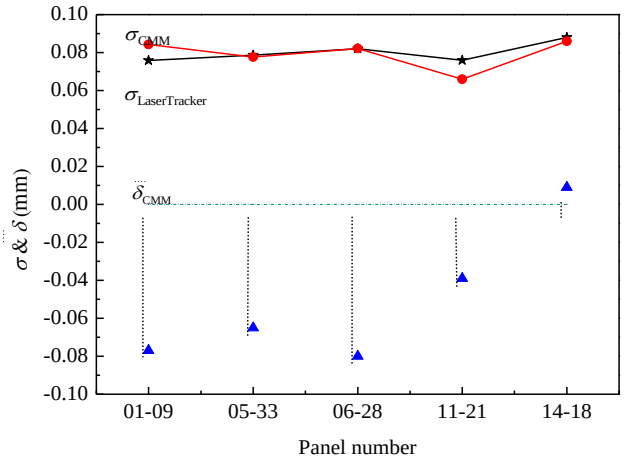

Fig. 6 The RMS value σ and error average value $\bar{\delta}$ of five panels. $\bar{\delta}_{CMM}$ are shown as Figure 7 and $\bar{\delta}_{LaserTracker}$ are zero.

Comparison between Figure 7(a) and 7(b) gives a clue that the maximum of the absolute value of δ derived from the CMM is in general larger than those from the laser tracker. A possible reason is that the σ_{CMM} contains a systematic error of the installation of the reference points. The whole reflector surface errors include single panel error, BUS error and installation error. Although the errors σ_{CMM} and δ_{CMM} are relatively larger, the condition in the factory is consistent with that on the BUS. Only the installation error needs to be adjusted if the single panel and BUS have been well calibrated. We caution that the overall errors σ_{LT} is smaller, but the condition of σ_{LT} measurement in the factory is not same with that on the BUS. In addition to the installing error, the adjustment has to take into account of panel error. Consequently, the CAD surface fitting method makes the panel installation/adjustment more difficult to achieve the same setting accuracy of the telescope.

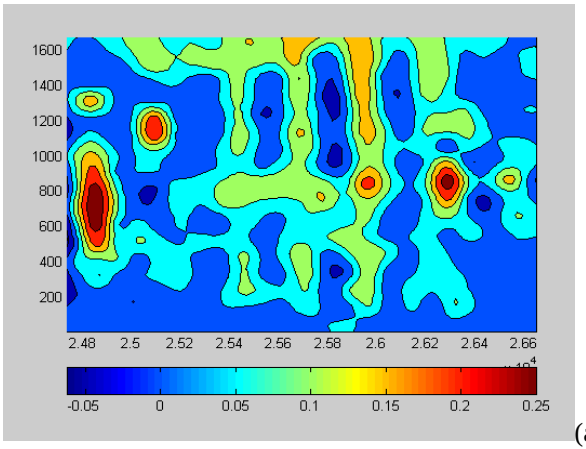

(a)

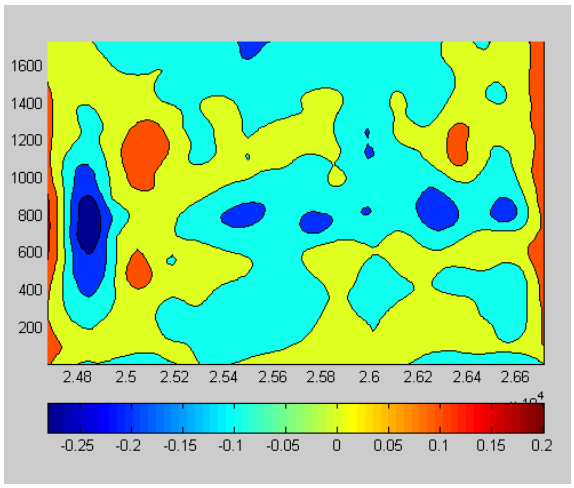

(b)

Fig. 7 (a) The panel deformation calculated through the common point coordinate transformation and (b) the CAD surface fitting method. The units of the horizontal and vertical coordinate axis are mm.

3. FEA of Panel Accuracy

The surface unevenness of panels under gravity, wind and temperature was conventionally analyzed by the finite element software. The analysis of gravity-induced deformation can deduce the manufacturing error from the measuring data.

The materials of the panel which are built using sheet glued in two longitudinal and several transversal *z*-shaped stiffeners are aluminum. The elastic module is typically 7.0×10^7Pa, the Poisson's ratio is 0.33, and the density is 0.0027kg/m^3. The *y* direction displacements of the four supporting points were constrained. According to the structure and deformation characteristics, shell63 and beam188 elements were adopted for the finite element analysis. When we meshed we should ensure the sheet and stiffener have common nodes on the intersected line. The sizes of the glue between the sheet and *z*-shaped stiffeners and the seam in the sheet and stiffeners were neglected when constructing the finite element model.

Figure 8 shows the contour of gravity-induced deformation under 90 ° elevation angle. The deformation accords with the deformation law of structure under uniform load that the profile is a parabola. The deformations in the middle are largest and the ones at the two edges are minimal. The surface accuracy of the panel is about 0.056mm.

The surface accuracies of the panel under elevation angle of 0 °, 15 °, 30 °, 45 °, 60 °, 75 ° and 90 ° are obtained. The results are shown as Figure 9 The rms value increases with the changing of elevation angle. Combining the measuring data with simulated data, we achieve that the manufacturing error is 0.065mm.

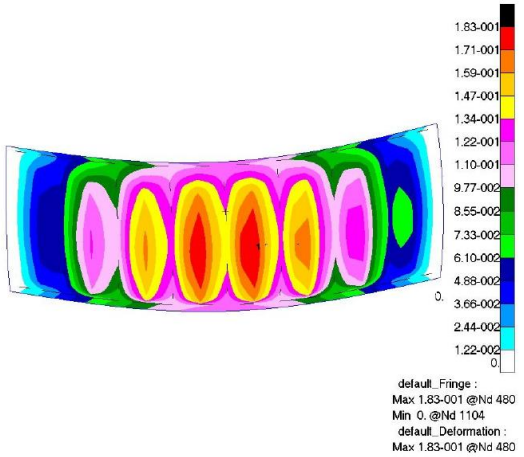

Fig. 8 The contour of gravity deformation under 90 ° elevation angle.

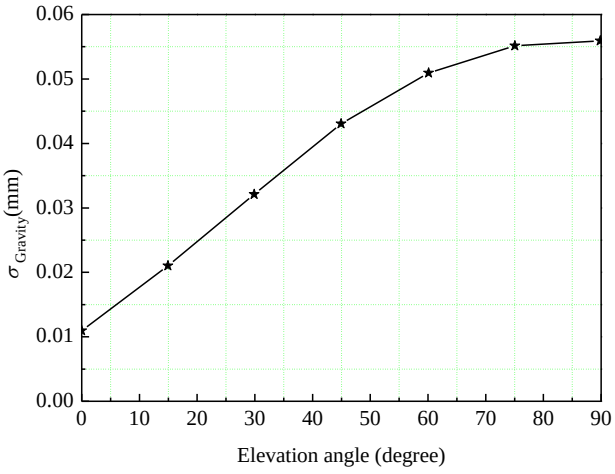

Fig. 9 The change of panel surface accuracy derived from gravity deformation at different elevation angles.

Temperature shift of 5℃ was applied on the

panel at the elevation angle 90°. The thermal deformation contour is shown as Figure 10. The deformation is uniform within the reflector surface and only becomes larger in the vicinity of the edge. The uncertainty of the panel surface accuracy induced by temperature change is 0.011mm. There are some arguments that the thermal-induced deformation is the case of the above FEA. In fact, the panel and the BUS are made of different materials (aluminum and steel). When the panels are constrained by the BUS, a uniform temperature change of the BUS and the panels causes panel buckling. The buckling amplitude Δz_{max} is derived by Christiansen & Högbom[12]

$$\Delta z_{\max} \approx 0.6l\left[\left(\alpha_{\mathrm{p}}-\alpha_{\mathrm{BUS}}\right)\Delta T\right]^{1/2} \quad (5)$$

where l is the panel length; α_{p} and α_{BUS} are the thermal expansion coefficients of the panel and BUS, respectively. According to the parameters of the panel and BUS we used, Δz_{max} is about 0.112mm and the rms value is $\sigma = \Delta z_{max}/3 = 0.037$mm. As a result, the change of surface accuracy is a little larger after the panel is constrained by the BUS.

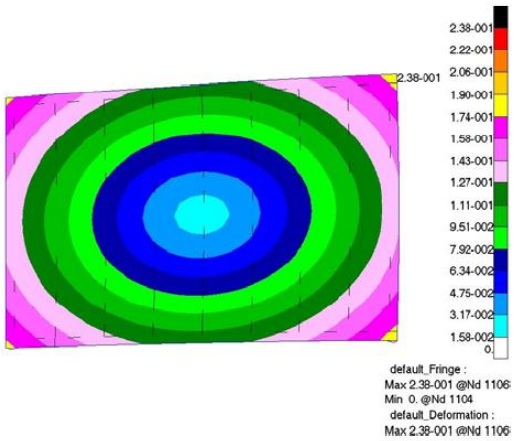

Fig. 10 The contour of thermal-induced deformation under 90°elevation angle.

We considered the effect of the vertical wind of 10m/s on the panel accuracy. Assuming a uniform wind load, it is calculated following the formula: [13]

$$F = C_{\mathrm{F}} qA \quad (6)$$

where C_{F} is the wind power coefficient; q=1/16v^2 is the dynamic pressure and v is the wind speed; A is the characteristic area. From (6), we determined F of 36N/m^2. The deformation contour is shown as Figure 11. Accordingly, the wind-induced uncertainty is 0.046mm.

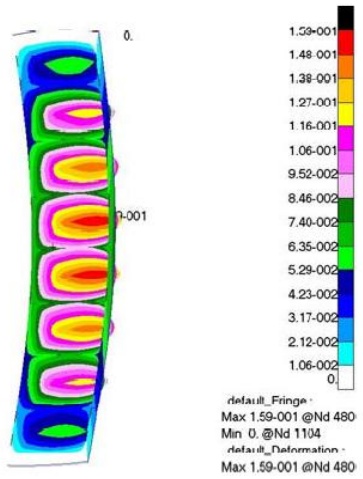

Fig. 11 The contour of wind-induced deformation under 90°elevation angle.

Table 1 lists the accuracy budgets resulted from different factors. Obviously, the manufacturing and gravity-induced errors are the primary error sources. These two kinds of errors are repeatable, which can be modeled and compensated by the active surface system. In principle, the manufacturing error could be further improved by enhancing the manufacturing process and by modifying molds. Wind- and thermal-induced errors have instantaneous and uncertain characteristics; they are not able to be fit with a solid model, and need intense monitoring and on-line calibration.

TABLE 1
ACCURACY BUDGET

Error source	RMS(mm)	Remark
Manufacturing	0.065	None
Gravity	0.056	Normal
Wind	0.046	10m/s normal
Thermal	0.037	5℃ temperature difference

4. Experiment and FEA of Concentrated Load on the Panel

It is inevitable to step on the panel during installing and servicing. Accordingly, it is necessary to analyze if it is elastic deformation when people step on the panel. In this paper, we obtain the deformation by experiment and simulation.

The experiment is shown as Figure 12. One people steps on the middle of the panel and dial

indicators are placed at the four corners and under the position of the people. The weight of the people is 70kg. The dial indicators show that the deformation in the middle of the panel is 0.71mm, the horizontal deformations of the supporting bolts are zero and the vertical deformation is 0.027mm.

The above experiment is simulated using finite element software. The establishment of the finite element model is similar in section 3 and only the load is different. The deformation of the panel in the position of concentrated load is 0.67mm.

The comparison error between the experiment and simulation is 5.6%. The stress of the maximum deformation point is $\sigma = E\ \varepsilon$ = 49.7MPa < $[\sigma]$. Therefore, the panel is elastic deformation under 70kg concentrated load. The experimental result show that the dial indicator is zero after the people left the panel.

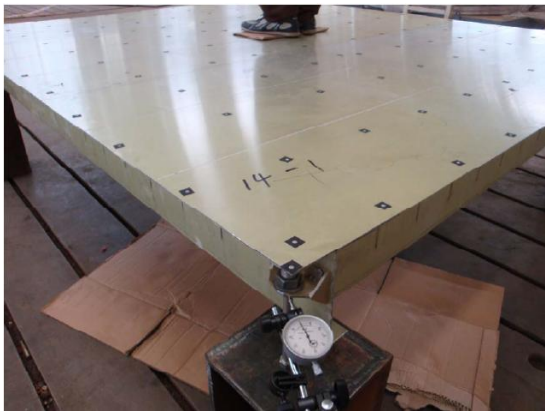

Fig. 12 The experiment of concentrated load applied on the panel.

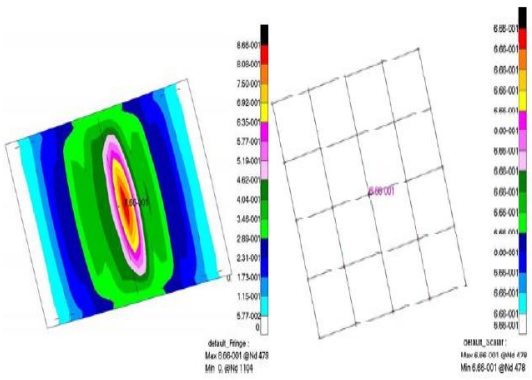

Fig. 13 The contour of deformation induced by concentrated load under 90 °elevation angle.

5. Conclusion

The panel surface accuracy of Sh65RT was measured independently with two different instruments and techniques, the CMM and laser tracker. The rms uncertainties obtained from the two approaches show excellent consistency. The ideal whole reflector surface accuracy will be achieved by repeated measurement and adjustment. The work condition of the CMM method in factory is more coincident with that on the BUS. Only four reference points of each panel need to be measured to compensate the installation errors. In contrast, the four adjusting points are not zero when the laser tracker method is used. Not only the four adjusting points but also the points on the panel need to be measured. The evaluation of the effects of wind, temperature, gravity and manufacturing error on the panel surface accuracy with the FEA software suggests that the latter two factors are of the primary care. The accuracy budget in this study offers a useful reference for other large antennas. The result of panel deformation under concentrated load shows that there is not plastic deformation when people of weight below 70kg installs and remedies the panel. But, people should prefer to pull on big shoes to distribute the pressure. The accuracies of single panels under different cases totally satisfy the design requirement, which assures the accuracy of primary reflector surface (less than 0.6mm).

We hope the experts and correlated organization can define the criterion of antenna structure design, *i.e.* the definition of panel surface accuracy and determination of the grade of wind speed and temperature shift according to different accuracy requirement.

Acknowledgment

This work was supported in part by the National Natural Science Foundation of China (Grant NO. Y347201001), Science and Technology Commission of Shanghai Municipality (08DZ1160100), and Knowledge Innovation Program of the Chinese Academy of Sciences (KJCX-YW-18). We appreciate the collaboration with Shanghai Shen Mo Die & Mold Manufacturing Co. Ltd**.** We thank Profs. Zhihan Qian (SHAO) and Dr. King Lee (NRAO) for the guidance.

References

[1] R. M. Prestage, et al., The Green Bank telescope, *IEEE Proceeding*, 2009, pp. 1382-1390.

[2] R. Wielebinshi, The Effelsberg 100-m radio telescope, *Naturwissenschaften*, vol.58, 1971, pp. 109-116.

[3] E. Cenacchi. SRT Project Book. Available: http://www.ca.astro.it/srt/project-book/index.htm
[4] A. Orfei, Updates on SRT, the Sardinia radio telescope, *in 8th Radionet Eng. Forum*, Yebes, 2008, pp.1-40.
[5] J. M. Hollis, P. R. Jewell, F. J. Lovas, and A. Remijan. Green Bank telescope observations of interstellar Glycolaldehyde: Low-temperature sugar, *The Astrophysical Journal*, 2004, pp. 45-48.
[6] S. Cichowolski, E. M. Arnal. An Effelsberg HI study of the ISM around WR 126, WR 154 and WR 155, *A&A*, vol 414, 2004, pp. 203-209.
[7] G. Zacchiroli, et al., The panels for primary and secondary mirror reectors and the Active Surface System for the new Sardinia Radio Telescope, *Mem. S.A.It. Suppl*., vol. 10, 2006, pp. 126-130.
[8] Jr. Hoagg, et al. Method for fabricating antenna reflector panels, United States Patent,1991, pp. 1-7.
[9] D. H. Parker, J. M. Payne, J. W. Shelton, and T. L. Weadon. Instrument for setting radio telescope surfaces, *GBT MEMO* 206, pp. 1-4.
[10] H. Kutoglu, C. Mekik, H. Akcin. Effects of errors in coordinates on transformation parameters, *J. Surv. Eng.*, vol. 129, 2003, pp. 91–94.
[11] Z. C. Li, G. Y. Li, C. Jin. On the data processing methods of surface antenna's inspection, *FIG XXII International Congress*, 2002, pp.1-9.
[12] W. N. Christiansen, J. A. Högbom. Radiotelescopes, Cambridge University Press, 1985.
[13] Z. G. Zhu, S. H. Ye. Antenna structure design, The National Defence Industry Press, 1980.